Mechanical Technology and Engineering Insights

www.mtei.reapress.com

Mech. Technol. Eng. Insights . Vol. 1, No. 3 (2024) 180–186.

Paper Type: Original Article

Multi-Objective Structural Optimization of a Large- Effect of Welding Current and Voltage on Weld Defects and Corrosion Resistance of HF-ERW ST37 Steel Pipes

Milad Hemmatnezhad[1,*], Sahar Hatami Pour[2]

[1] Department of Mechanical Engineering, Takestan Branch, Islamic Azad University, Takestan, Iran; m_hemmatnezhad@yahoo.com.

[2] Department of Industrial Engineering, Ayandegan University, Tonekabon, Iran; saharhatamipour01@gmail.com.

Citation:

Received: 12 June 2024 *Revised: 22 Auguste 2024* *Accepted: 24 October 2024*	Hemmatnezhad, M., & Hatami Pour, S. (2024). Effect of welding current and voltage on weld defects and corrosion resistance of HF-ERW ST37 steel pipes. *Mechanical Technology and Engineering Insights, 1*(3), 180-186.

Abstract

The High-Frequency Welding (HFW) process is one of the most frequently employed fabrication techniques to manufacture longitudinally welded steel pipes in pipeline transport for oil and gas transmission applications. In this study, the impact of current strength and electrical potential on radiographic features and corrosion properties of HFW-steel ST37 pipes was analyzed. A 12 inches diameter ST37 steel pipe with a wall thickness of 6 mm was manufactured using the High-Frequency Electric Resistance Welding (HF-ERW) method by varying the current of welding between 1100 and 1130 A and keeping the frequency equal to 180 Hz. Radiography was performed to assess defectiveness and porosity structure. Also, electrochemical corrosion properties were studied using Tafel polarization curves in 3.5 wt.% NaCl medium. Electrochemical parameters, such as corrosion current density (icorr), corrosion potential (Ecorr), and polarization resistance (Rp), were obtained from Tafel polarograms using Stern–Geary equation. The radiography revealed that the increase in welding current and voltage led to a remarkable increase in porosity formation in welds owing to intensive heat exposure. The results of the electrochemical analysis show that the welds subjected to higher current intensities had a high corrosion current density and low polarization resistance, meaning a lower resistance to corrosion. The test sample with the highest porosity level performed poorly in terms of corrosion since pores and voids served as preferred locations of electrochemical corrosion and the entry of chloride ions into the metal matrix. The findings prove the importance of controlling HFW conditions to reduce corrosion in ST37 pipelines.

Keywords: High frequency welding, High-frequency electric resistance welding, ST37 steel, Radiographic evaluation, Weld porosity, Corrosion behavior, Tafel polarization, NaCl solution, Pipeline steel, Electrochemical corrosion.

1 | Introduction

Alloyed low-carbon steels have become common materials across many sectors, such as automobiles, the oil industry, pipelines, and aerospace, because of their favorable mechanical behavior, weldability, and lower

Corresponding Author: m_hemmatnezhad@yahoo.com

https://doi.org/10.48313/mtei.v1i3.66

prices [1]. Among those low-carbon steels, one type, ST37, is defined by DIN 17100 and has become one of the most common alloys used in the oil industry [2].

High-Frequency Welding (HFW) or High-Frequency Electric Resistance Welding (HF-ERW) is a crucial manufacturing technique for producing longitudinal seam pipes from steel strip. This technique involves applying high-frequency alternating current (100-400 kHz) to generate localized resistive heating at the edges of cold-formed steel strips, then forging the strip under pressure without filler metal. Some of the strengths of HF-ERW include reduced heat input, precise dimensions, higher efficiency, and shorter delivery time, among others, as explained in detail by Brito et al. [3].

HFW welds require careful, accurate adjustment of welding parameters to ensure high-quality welds and the integrity of the welds. As noted by some researchers, a frequency of 150 kHz, compression force of 4 marks, and Vee angle of 5° would provide the best mechanical results when using HF-ERW on API X52 microalloy steel joints [4].

Some research studies have examined how welding current affects weld performance, especially in low-carbon steels. For instance, Jannifar et al. [2] determined the impact of welding current on the corrosion resistance and hardness of ST37 steel welded joints (at 75, 85, and 95 amperes). As the welding current increased, corrosion resistance decreased, making the weld zone more susceptible to corrosion. The maximum corrosion rate was 0.10516 mm/year in samples with a welding current of 95 amperes, whereas the highest hardness was observed in the weld metal at 75 amperes [2].

The uncontrolled use of welding parameters can lead to weld defects. Non-Metallic Inclusions (NMIs) were named as a reason for defects appearing in High-Frequency Resistance-Welded (HFRW) joints. Kazakov et al. [5] conducted detailed research on the chemical composition and origin of NMIs in defects of pipe joints fabricated by HFW technology. As a result, the following conclusion was made: The composition of NMIs greatly differs since it comes from indigenous deoxidation products of the spinel type of MgO. Al_2O_3 (8%), products of steel modification due to calcium addition (62%), residues of mould flux (4%), and from other exogenous sources. Besides, Kazakov et al. [5] reported that hook cracks prevail among various defects in High-Frequency Induction Welded (HFIW) pipes and that there is a direct relation between NMIs along the weld bondline and the appearance of the mentioned crack.

Radiographic testing is commonly used for non-destructive testing of longitudinal welded pipes. At the same time, Shleenkov et al. [6] discovered that non-metallic inclusions of liquation strips appearing on the edge and falling into the welding area could be found in X-ray inspection, but are not recognized as defects. The misinterpretation results from the fact that the grooves' location within the zones of the welded joint corresponds to the X-ray diffraction spectra. In contrast, no such defects were found with other control procedures and metallographic studies [6].

The weld metal's corrosion resistance is a critical factor that dictates the pipeline's performance. The welding process causes localized heating and solidification, which give the weld metal different properties, leading to its corrosion. Electric-resistance-welded pipes made of carbon and low-alloy steels enriched with sulfur exhibit grooving corrosion under neutral-salt-water conditions; this localized corrosion occurs at the weld zone [7]. The potential corrosion rate of grooving is evaluated using an accelerated potentiostatic test, with sulfur concentration being an important factor in assessing susceptibility to this type of corrosion [7]. On the other hand, HFI welded line pipes made of carbon and low-alloy steels resist groove corrosion due to their low sulfur content [7].

Additional research has also examined the effect of microstructure on toughness in HFI-welded pipes and analyzed different parameters, including microstructure, grain size, precipitates, hardness, inclusions, and texture, to correlate weld microstructure with toughness of the HFI-welded joint [8].

A case study by Tyrala and Pawlowski [9] focused on a premature corrosion failure of an HF induction seam-welded steel pipe used in a central heating system. Microscopic investigation by these authors showed that the failure was due to a problem associated with the HF induction welding process, namely, a so-called cast weld, a weld line containing a large amount of iron oxides due to poor ejection of molten metal at the bond line. Tyrala and Pawlowski [9] noted that the pipe failed by longitudinal cracking less than 2 years after operation due to a weld-line failure. It can thus be concluded that weld defects such as oxides trapped in the HF-ERW seam cause longitudinal cracking during service.

Pawłowski et al. [10], through further research on seam-welded galvanized steel cold-water pipes, revealed that premature failure due to corrosion occurs within 18-24 months of installation in service. In a separate study by Tyrała and Pawłowski [11], pitting corrosion was observed solely in regions of seam-welded L235 steel pipes with many microvoids, suggesting that high levels of trapped hydrogen in these pipes could lead to early failure. These findings reveal the importance of welding defects, especially oxide inclusions, in reducing the lifespan of steel pipes.

There is substantial evidence suggesting Post-Weld Heat Treatment (PWHT) as an efficient approach to improve weld properties. Some novel PWHTs involving normalization, quenching, and tempering procedures have been successfully applied to improve toughness in high-frequency electrical resistance-welded welds [12]. In the case of API X60 steels, quenching and tempering heat treatment (600ºC/30min) was successful in increasing absorbed energy twofold compared to commercial treatments, while maintaining the hardness and ultimate strength of the weld at 33J, compared to commercial heat treatments at -25ºC (17J) [12].

Due to the high degree of applicability of ST37 steel in various industries as well as the necessity for good weldability, it has become necessary to conduct a thorough study on how HFW parameters, especially current density and voltage, affect the creation of such defects as can be revealed using radiography and, subsequently, their strength and durability characteristics. The present research focuses on filling this knowledge gap by studying the aforementioned factors in the case of ST37 steel pipes manufactured using HFW.

2 | Materials and Methods

For the current work, a 12-inch steel pipe with a 6 mm wall thickness, manufactured from ST37 low-carbon steel, was used (*Fig. 1*). The steel pipe was produced using the HFW technique via induction current transfer in a Siemens welding facility in Germany. The HFW process was performed at a constant frequency of 180 Hz; however, varying current and potential values were applied for the conditions specified in *Table 1*. The pipes were manufactured in accordance with API specifications. The chemical analysis of the ST37 steel sample was conducted using an Optical Emission Spectrometric technique, as shown in *Table 2*.

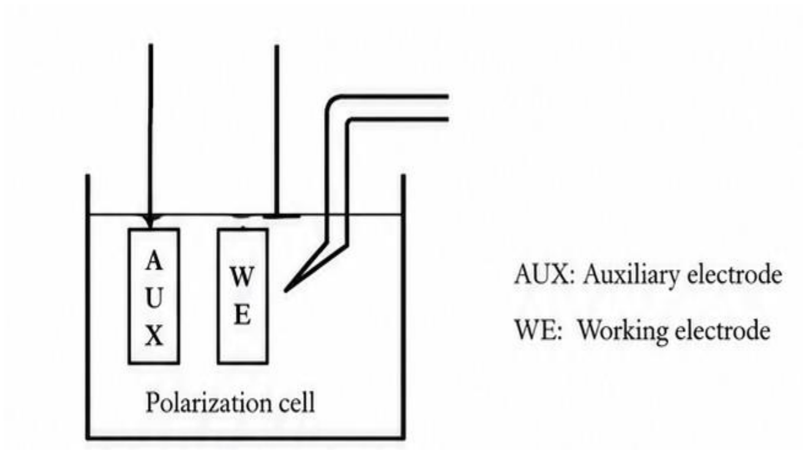

Fig. 1. Schematic illustration of the mounting configuration of the welded specimen and its immersion in the electrolyte solution for the Tafel polarization test.

Table 1. Welding parameters of HF-Welded ST37 steel pipe samples produced under different current intensities.

Sample No.	Diameter (inch)	Grade	Thickness (mm)	Frequency (Hz)	Current (A)	Voltage (V)	Welding Speed (m/s)
Sample 1	12	API	6	180	1100	312	7
Sample 2	12	API	6	180	1115	320	7
Sample 3	12	API	6	180	1120	325	7
Sample 4	12	API	6	180	1125	330	7
Sample 5	12	API	6	180	1130	335	7

Table 2. Average chemical composition of ST37 steel samples (wt.%).

Fe (%)	C (%)	Si (%)	Mn (%)	P (%)	S (%)	Cr (%)	Ni (%)	Mo (%)	Cu (%)
Balance	0.107%	0.0372%	0.577%	0.0143%	0.0064%	0.003%	0.0171%	0.005%	0.0214%
Co (%)	V (%)	Ti (%)	Pb (%)	Bi (%)	Al (%)	As (%)	Sn (%)	Ca (%)	Nb (%)
0.008%	0.002%	0.002%	0.025%	0.030%	0.050%	0.009%	0.003%	0.001%	0.002%

Radiographic images of the weld cross-sections were taken and analyzed using an industrial radiographic viewer system to determine porosity distribution and weld defects. Radiographic examination was performed to detect discontinuities in the metal, such as gas porosity and high-penetration defects, that were created during the HFW process.

Circular specimens with a surface area of 1 cm² were cut so that the weld line was at the center of each specimen for measuring corrosion rate using electrochemical corrosion measurement. The corrosion properties of the HFW specimens were tested using electrochemical Tafel polarization. Experiments were carried out on a standard three-electrode electrochemical cell immersed in 3.5% NaCl solution at 25 °C. A Saturated Calomel Electrode (SCE) was used as the reference electrode, graphite as the Auxiliary Electrode (AE), and an HFW specimen as the Working Electrode (WE).

Electrochemical tests were conducted on a state-of-the-art potentiostat/galvanostat instrument (EG&G PARSTAT 2273) that utilized the PowerSuite software from AMETEK. Prior to the polarization test, the samples were soaked in the electrolytic solution for 30 minutes to achieve a steady (OCP). Electrochemical Tafel polarization studies were performed over a potential range of -0.25 V to 0.5 V with respect to OCP at a scan rate of 1 mV s^{-1}.

The values of I_{corr} (corrosion current density), E_{corr} (corrosion potential), β_α (anodic Tafel slope), and β_c (cathodic Tafel slope) were determined from the polarization curves through the use of the PowerSuite electrochemical analysis software. The corrosion resistance properties were assessed using the Stern–Geary equation, which relates polarization resistance and corrosion current density as follows.:

$$i_{corr} = \left[\frac{1}{2.303\ R_p}\right]\left[\frac{\beta_\alpha . \beta_c}{\beta_\alpha + \beta_c}\right], \quad (1)$$

where i_{corr} is the corrosion current density (A/cm^2), R_p is the polarization resistance ($\Omega\ cm^2$), and β_α, β_c represent the anodic and cathodic Tafel slopes, respectively.

The corrosion current density was determined by extrapolating the linear Tafel regions of both anodic and cathodic branches to the corrosion potential. In the polarization curves, the anodic and cathodic regions exhibited linear behavior at approximately ±50 mV relative to the open circuit potential, corresponding to the Tafel regions.

3 | Results and Discussion

3.1 | Radiographic Analysis

Fig. 2 presents the radiographic images obtained from the welded samples. As observed, the weld regions contain noticeable porosity defects accompanied by excessive penetration, indicating that these defects were generated under high heat input conditions during the welding process. The observed pores were randomly distributed throughout the weld region and can therefore be classified as dispersed porosity.

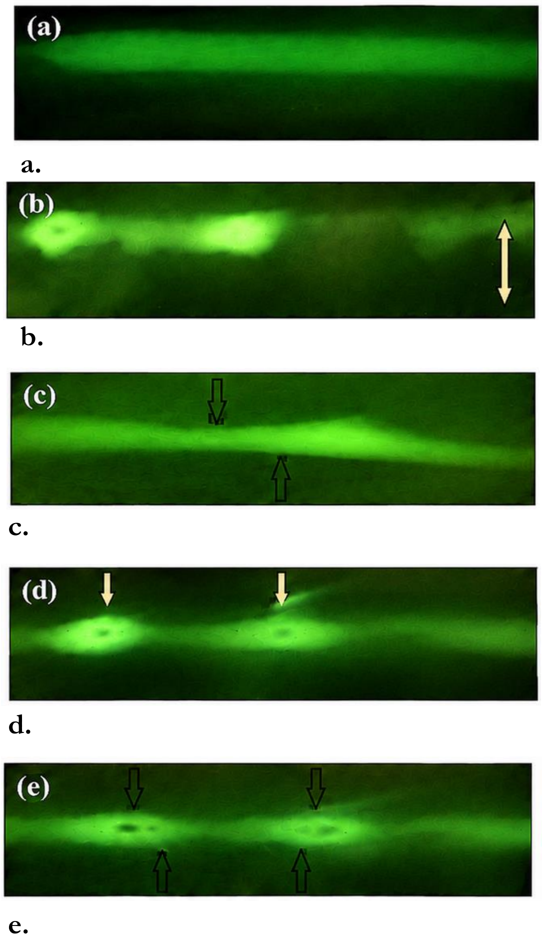

Fig. 2. Radiographic images obtained from the welded samples under different welding current conditions; a. 1100 A, b. 1115 A, c. 1120 A, d. 1125 A, and e. 1130 A.

The radiographic results clearly indicate that increasing the welding current and electrical potential resulted in a significant increase in porosity in the weld zone. The formation of such defects is mainly associated with excessive heat input during welding. At elevated temperatures, the solubility of hydrogen in molten metal increases considerably. During rapid solidification, excess dissolved hydrogen does not have sufficient time to escape from the molten weld pool. Consequently, it becomes trapped in the form of gas pores throughout the weld metal.

Furthermore, surface contamination and residual oil or grease on the steel coil surface may also contribute to hydrogen generation during welding, thereby intensifying porosity formation. When the hydrogen content in the molten weld exceeds the solubility limit, severe gas evolution occurs within the weld pool. Under these conditions, pores tend to nucleate and grow near the weld/base metal interface because this region experiences the shortest molten-state duration during solidification. As supersaturation increases, larger cavities and clustered porosity defects form in the weld region.

3.2 | Electrochemical Corrosion Results

Fig. 3 illustrates the Tafel polarization curves of the welded samples containing the minimum and maximum porosity levels immersed in a 3.5 wt, % NaCl solution. The electrochemical parameters extracted from the polarization curves are summarized in *Table 3*.

The corrosion parameters, including corrosion potential (E_{corr}), corrosion current density (i_{corri}), anodic Tafel slope (β_α), and cathodic Tafel slope (β_c), were obtained using PowerSuite electrochemical analysis software. Corrosion resistance was evaluated using the Stern–Geary equation.

The obtained polarization curves demonstrate that the sample welded at a lower current (1130 A) exhibited higher corrosion resistance than the sample welded at a higher current (1130 A). This behavior can be attributed to the increased porosity in the weld region at higher heat inputs. The pores and micro voids formed during welding act as preferential sites for localized electrochemical attack and facilitate the penetration of chloride ions into the weld metal.

In addition, porosity increases the effective active surface area exposed to the corrosive environment and accelerates localized dissolution. Consequently, the welded specimen produced at higher current intensity exhibited a higher corrosion current density and lower polarization resistance, indicating inferior corrosion resistance compared with the specimen welded at lower current intensity.

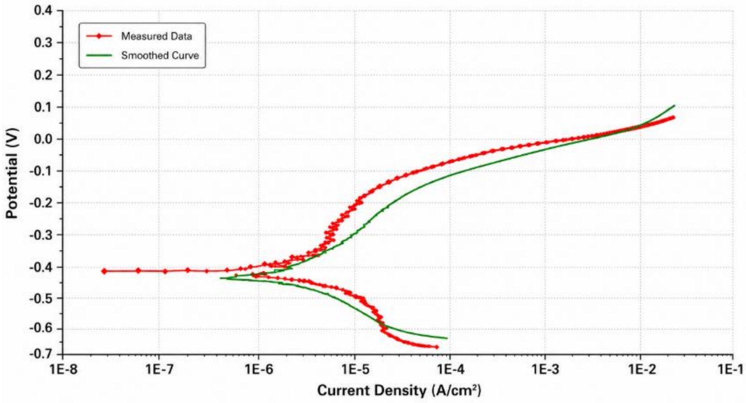

Fig. 3. Tafel polarization curves of the welded samples with the minimum and maximum weld porosity immersed in 3.5 wt.% NaCl solution.

Table 3. Corrosion potential, corrosion current density, polarization resistance, and Tafel slopes obtained from potential dynamic polarization diagrams.

Sample Type	β_α (mV/decade)	β_c (mV/decade)	E_{corr} (mV)	I_{corr} ($\mu A \cdot cm^{-2}$)	R_p ($\Omega \cdot cm^2$)
Sample with minimum porosity (Sample 1)	45.81	41.87	−447	0.45	11.2×10^4
Sample with maximum porosity (Sample 5)	87.992	58.23	−478.85	0.806	1.89×10^4

4 | Conclusion

In this work, the effects of welding current and voltage on the radiographic properties and corrosion resistance of HF-welded ST37 steel pipes have been investigated. Radiographic examination of the weld has shown that increasing the welding current and voltage resulted in a noticeable increase in dispersed porosity in the weld zone. The formation of these defects was due to high heat input during the welding process. Increased heat input increased hydrogen solubility in the melted weld and led to the formation of pores during cooling.

To assess the electrochemical corrosion resistance of the specimens, Tafel polarization curves in 3.5 wt.% NaCl solution has been constructed. According to the results, increased porosity in the weld zones was accompanied by elevated corrosion current density and low polarization resistance. On the other hand, the sample welded at a lower current showed better corrosion resistance than the sample welded at a higher current. This implies that high current intensity during welding is detrimental to weld quality and corrosion resistance in HF-ERW ST37 steel pipes. All in all, the results of this study clearly indicate that optimizing HFW process parameters is critical for preventing weld defects and improving the corrosion resistance of the pipe used in corrosive conditions.

Conflict of Interest

The authors declare that they have no competing interests.

Data Availability

The data supporting the findings of this study are available within the article.

Funding

This research did not receive any external funding.

References

[1] Llewellyn, D., & Hudd, R. (1998). *Steels: Metallurgy and applications*. Elsevier. https://www.amazon.com/s?k=9780080517766&i=stripbooks&linkCode=qs

[2] Jannifar, A., Ichsan, T. A., Nurdin, H., Mukhtar, F., & Wahyudi, W. (2019). Welding current effect of welded joints of base metal st37 on characteristics: Corrosion rate and hardness. *IOP conference series: earth and environmental science*, *268*(1), 12167. https://doi.org/10.1088/1755-1315/268/1/012167

[3] Ravikiran, K., Xu, P., & Li, L. (2024). A critical review on high-frequency electric-resistance welding of steel linepipe. *Journal of manufacturing processes*, *124*, 753–777. https://doi.org/10.1016/j.jmapro.2024.06.046

[4] Sabzi, M., Kianpour-Barjoie, A., Ghobeiti-Hasab, M., & Dezfuli, S. M. (2018). Effect of high-frequency electric resistance welding (HF-ERW) parameters on metallurgical transformations and tensile properties of API X52 microalloy steel welding joint. *Archives of metallurgy and materials*, *63*(4), 1693–1699. https://doi.org/10.24425/amm.2018.125094

[5] Kazakov, A. A., Kiselev, D. V, Murysev, V. A., & Rybalchenko, I. V. (2022). Non-metallic inclusions and hook cracks of high-frequency induction welded pipes. *CIS Iron and steel review*, *24*, 49–59. https://doi.org/10.17580/cisisr.2022.02.08

[6] Shleenkov, A. S., Novgorodov, D. V, & Konovalchuk, V. O. (2022). Study of defects of longitudinal welded pipe. *AIP conference proceedings*, *2503*(1), 50080. https://doi.org/10.1063/5.0099909

[7] Duran, C., Triess, E., & Herbsleb, G. (1986). The resistance of high frequency inductive welded pipe to grooving corrosion in salt water. *Mater. performance;(united states)*, *25*(9), 41. https://trid.trb.org/view/429765

[8] Güngör, O. E., Yan, P., Thibaux, P., Liebeherr, M., Bhadeshia, H. K. D. H., & Quidort, D. (2010). Investigations into the microstructure–toughness relation in high frequency induction welded pipes. In *International pipeline conference* (Vol. 44212, pp. 577-585). International Pipeline Conference. 10.1115/IPC2010-31372

[9] Tyrala, D., & Pawlowski, B. (2021). Failure analysis of premature corrosion of HF seam-welded steel pipe in central heating system. *Journal of failure analysis and prevention*, *21*(3), 772–778. https://doi.org/10.1007/s11668-021-01134-6

[10] Pawłowski, B., Tyrala, D., & Pilch, M. (2020). Metallographic investigations of the premature corrosion failure of steel seam-welded galvanized cold water pipes. *Journal of failure analysis and prevention*, *20*(1), 9–14. https://doi.org/10.1007/s11668-020-00803-2

[11] Tyrała, D., & Pawłowski, B. (2022). Microstructural aspects of premature pitting corrosion of steel pipe–case study. *Journal of failure analysis and prevention*, *22*(6), 2147–2153. https://doi.org/10.1007/s11668-022-01530-6

[12] Khalaj, G., Pouraliakbar, H., Jandaghi, M. R., & Gholami, A. (2017). Microalloyed steel welds by HF-ERW technique: Novel PWHT cycles, microstructure evolution and mechanical properties enhancement. *International journal of pressure vessels and piping*, *152*, 15–26. https://doi.org/10.1016/j.ijpvp.2017.04.003